pubs.acs.org/Biomac

Article

Synthesis of an Effective Flame-Retardant Hydrogel for Skin Protection Using Xanthan Gum and Resorcinol Bis(diphenyl phosphate)-Coated Starch

Yuan Xue,* Fan Yang, Juyi Li, Xianghao Zuo, Bole Pan, Mingkang Li, Lisa Quinto, Jalaj Mehta, Lauren Stiefel, Conor Kimmey, Yuval Eshed, Eyal Zussman, Marcia Simon, and Miriam Rafailovich*

Cite This: https://doi.org/10.1021/acs.biomac.1c00804

Read Online

ACCESS | Metrics & More | Article Recommendations

ABSTRACT: We report on the production of a flame-resistant xanthan gum (XG)-based hydrogel formulation, which could be directly applied onto the skin for protection against burning projectiles. The hydrogel cream represents an efficient use of XG and starch, both of which are biodegradable, reusable natural materials and are also GRAS-certified. The flame-retardant agent resorcinol bis(diphenyl phosphate) (RDP) was shown to be nontoxic to cells in vitro when adsorbed directly onto the starch delivery vehicle. Three hydrogel formulations were studied, the pure XG hydrogel, commercial FireIce hydrogel, and RDP-XG/RDP-starch hydrogel. After application of a direct flame for 150 s, the RDP-XG/RDP-starch hydrogel produced a thick char layer, which was easily removed, showing undamaged chicken skin and tissue underneath. In contrast, complete burning of skin and tissue was observed on untreated control samples and those covered with FireIce and pure XG hydrogels. The thermal protective performance test was also performed, where the heat transfer was measured as a function of time for all three hydrogels. The RDP-XG/RDP-starch hydrogel was able to prolong the protection time before obtaining a second-degree burn for 103 s, which is double that for FireIce and triple that for the pure XG hydrogel. The model proposed involves endothermic reactions, producing char and burning "cold", as opposed to simply relying on the adsorbed water in the hydrogel for burn protection.

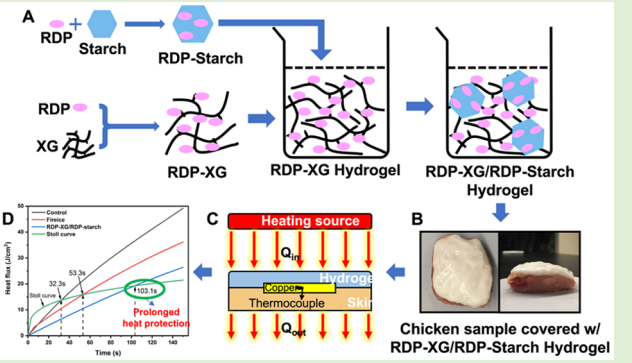

1. INTRODUCTION

Research has shown that the majority of burn injuries for firefighters rushing in to fight open fires occur on the face and nearby areas.[1,2] One of the causes for injuries is exposure to fire products, such as flying embers and other projectiles from the fires that come in contact with exposed skin or protective clothing that transfer the heat. Protective gear for firefighters is effective and highly developed, but many remove the facial component due to heat and discomfort. Hence, in addition to the standard protective equipment, there is currently a great demand for materials that are comfortable, do not restrain motion, and can be applied easily and directly onto the exposed areas. Hydrogel materials offer an attractive option for this application.

High biocompatibility, highly controllable texture, and self-healing properties have enabled hydrogels to be extensively used in the biomedical applications,[3,4] such as soft contact lenses,[5] drug delivery systems,[6,7] and wound dressings.[8] In particular, hydrogels have been extensively applied to retain hydration, deliver antibiotics, and permit healing in burn injuries.[9,10] Hence, we propose that in addition to treatment, these materials may also be appropriate for prevention of burn injuries. Hydrogels constitute a group of polymeric materials in which the hydrophilic structure renders them capable of sequestering large amounts of water within three dimensional networks, where tortuosity also inhibits evaporation. Hence, the current designs for flame-retardant hydrogels rely on the high water content to act as the main flame retardant. The current trend has also been able to produce thick gel sheets, which are sufficiently hard, so that they can be sewn into fabrics, such as the flame-retardant polyacrylamide-alginate hybrid hydrogel developed by Illeperuma et al.,[11] which was meant to be applied as a fire-resistant hydrogel-fabric laminate. However, since the material relies mostly on hydration to

Received: June 24, 2021
Revised: September 10, 2021

extinguish fires, the laminate thickness required to provide effective protection is relatively large, increasing the rigidity of the construct, resulting in motion limitation for the wearer. An alternative approach is the introduction of flame-retardant compounds, which act synergistically with the hydrogel polymer to rapidly extinguish fires. Furthermore, taking our cue from the cosmetic industry, flame-retardant materials could be formulated into creams that are easily applied and originate from natural sources, such that they are generally recognized as safe (GRAS) rated by FDA and will not irritate when placed in contact with the skin.

There are numerous natural hydrogels, which are abundant and economical and do not require toxic cross-linking agents.[12,13] Discovered in the 1950s, xanthan gum (XG) is a natural biopolymer that consists of a repeated unit formed by two mannose units, two glucose units, and a glucuronic unit.[14] Due to its nontoxicity, high thermal stability, and low flammability, XG has a wide range of applications in industries, such as suspension stabilizers, thickening agents, and controlled drug delivery purposes.[15] Furthermore, XG is well known as a shear thinning agent, which makes it easy to spread. Previous research showed that mixing starch into XG improves the stability, viscosity, and mechanical performances of the gel.[16,17] Leone et al. prepared hydrogels by mixing poly(vinyl alcohol) and XG that demonstrated a superior heat capacity, making them a good candidate for the cross-linking agent of flame-retardant hydrogels.[18]

Resorcinol bis(diphenyl phosphate) (RDP) is a biodegradable phosphate that is found to be an effective flame retardant in readily charrable polymers in previous research.[19−21] It suppresses flames by acting as an acid precursor and acid precipitate to promote surface charring through esterification and dehydration.[22] RDP-coated cellulose or starch was shown to be effective in rendering polymeric materials flame retardant. Therefore, in this research, we formulated the flame-retardant XG hydrogel with the addition of RDP-coated starch. The synthesized hydrogel displayed outstanding flame-retardant properties and thermal protection against extensive heat. The rheology test showed that the hydrogel is shear thinning, which enabled it for quick and easy application. Since all materials used except for RDP were GRAS compliant, only RDP/Starch was further tested for toxicity. While RDP in the liquid form had a well-defined IC50, no damage to skin cells was detected when it was adsorbed onto starch. Hence, we show here how the combination of these factors can be used to formulate an effective hydrogel cream, which can be easily applied on the skin to reduce burn-related injuries.

2. MATERIALS AND METHODS

2.1. Materials. XG powder was purchased from Judee's (Ohio, USA). The Fyrolflex RDP was provided by Israel Chemicals Ltd. Corn-based starch was supplied by National Starch.

2.2. Preparation of RDP-Coated Starch and RDP-Coated XG. In order to prepare RDP-coated starch (RDP-starch), 30 wt % of RDP was first poured into a beaker and then placed on a hot plate stirrer at 80 °C. The RDP was heated until the viscosity decreased enough for easy movement of the stir bar. Then, 70 wt % of starch was added into the RDP and manually stirred until all RDP was absorbed by starch. The mixture was kept under 50 °C for 10 min in a Hotpack vacuum oven. The mixed powder was then centrifuged three times using an ARE-250 THINKY centrifuge for further homogenization. The centrifuge was set at a speed of 750 rpm for 5 min. The product was transferred back into the beaker and kept in a Hotpack vacuum oven at 60 °C for 24 h to remove all remaining moisture. The RDP-coated xanthan gum (RDP-XG) was prepared following the same procedure as described for preparation of RDP-starch, with an RDP/XG weight ratio of 3:7.

2.3. Hydrogel Preparation. Powders of XG and RDP-XG were added to deionized water with a weight ratio of 2.5 wt %. The solutions were stirred at 380 rpm overnight at 45 °C to fully develop into hydrogels. The beaker was covered with parafilm to minimize evaporation during overnight stirring. The XG/RDP-starch hydrogel and RDP-XG/RDP-starch hydrogel were prepared by adding 10 wt % of RDP-starch to the previously prepared XG hydrogel solution and RDP-XG hydrogel solution and then stirred at 380 rpm overnight to obtain the homogeneous solutions. Compositions of the hydrogel solutions used in this study are listed in Table 1.

Table 1. Formulations of Hydrogels Used in This Study

sample	XG (wt %)	RDP-XG (wt %)	RDP-starch (wt %)
XG	2.5	0	0
RDP-XG	0	2.5	0
XG/RDP-starch	2.5	0	10
RDP-XG/RDP-starch	0	2.5	10

2.4. Cell Culture. Primary human dermal fibroblasts were obtained from a 31-year-old Caucasian female (CF-31, Clonetics, San Diego, CA). Dulbecco's modified Eagle medium (DMEM) (Catalog No: 11885-084), Dulbecco's phosphate-buffered saline (Catalog No: 14190-250), penicillin−streptomycin solution (Pen/Strep) (Catalog No: 15140-112), fetal bovine serum (FBS) (Catalog No: SH30071.03), and 0.05% trypsin−EDTA (Catalog No: 25300-054) were purchased from Thermo Fisher Scientific. Alexa Flour 488 phalloidin and 4′6-diamidino-2-phenylindole (DAPI) were also obtained from Thermo Fisher Scientific.

CF-31 cells were routinely cultured in DMEM supplemented with 10% FBS and 1% Pen/Strep (full-DMEM), in an incubator set at 37 °C, 5% CO_2, and 95% humidity. Cell culture media were changed every 2 to 3 days. Starch and RDP/starch media were prepared by dispersing particles in full-DMEM with different concentrations. Before using, particle solutions were sonicated for 30 min and stirred, to break down particle clusters and help particles disperse homogeneously. For the RDP chemical study, RDP was added directly into the cell culture media.

To investigate cell proliferation, 8000 CF-31 cells were seeded in 24-well plates with full-DMEM. After incubation for 24 h, culture media were changed using full-DMEM and particle media, respectively. Cells were then counted using a hemocytometer on different days. To obtain cell morphology, we fixed the cells in 3.7% formaldehyde for 15 min and stained actin filaments with Alexa Fluor 488 phalloidin and nuclei with DAPI. After this, the cells were imaged under an EVOS cell imaging system.

2.5. Characterization Methods. *2.5.1. Flammability Test.* Chicken tissue samples with a dimension of 2 cm × 2 cm × 1 cm covered with hydrogels were subjected to the burning test for assessing the flammability of the hydrogels. The chicken tissue samples consist of two parts, the skin layer and the tissue layer. Hydrogels were applied onto the skin surface with a thickness of 2 mm. A thermocouple was pierced through the tissue layer until the tip reaches right underneath the skin layer. All samples were burned with a propane torch for 150 s. The thermocouple was connected to a thermal meter, and the temperature change of the chicken tissue sample during burning was recorded as a function of time. An infrared camera was also used to record the thermal imaging of the burning process.

2.5.2. Thermogravimetric Analysis (TGA). TGA tests were conducted with a TA instrument TGA Q500. Tests were run from 35 to 750 °C at a heat rate of 10 °C/min. All tests were done in a nitrogen atmosphere, and the weight loss vs temperature curve and the derivative of the weight loss curve were obtained.

https://doi.org/10.1021/acs.biomac.1c00804
Biomacromolecules XXXX, XXX, XXX−XXX

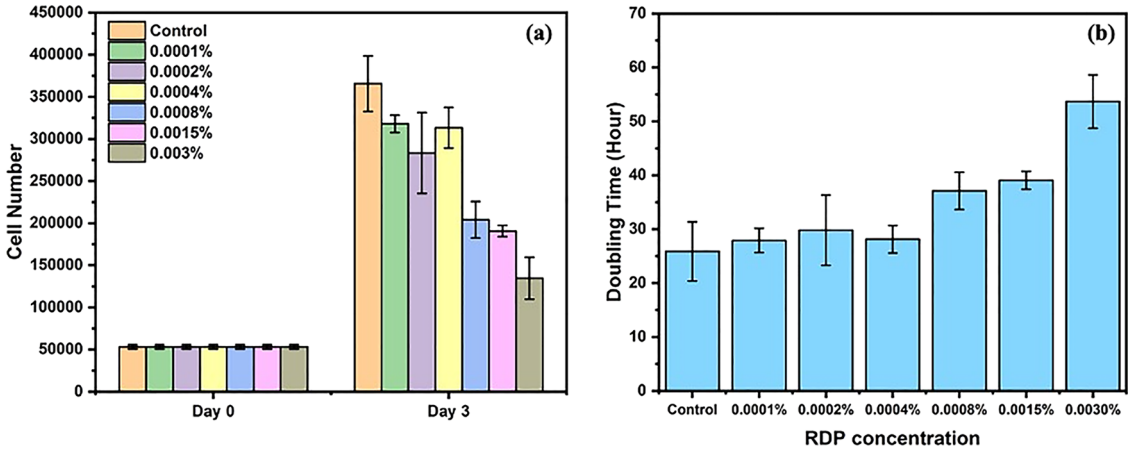

Figure 1. Human dermal fibroblast cell proliferation study to analysis the toxicity of RDP: (a) cell number and (b) doubling time of cells grown on media with different concentrations of RDP.

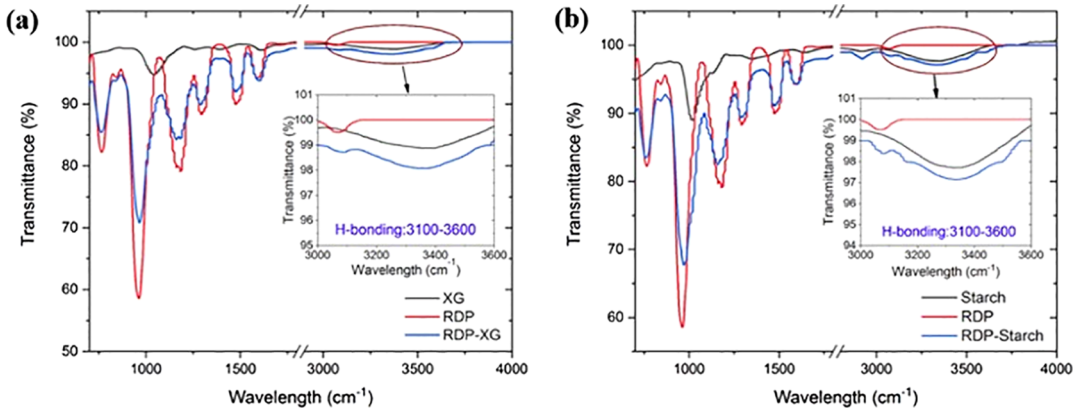

Figure 2. FTIR spectra of XG, Starch, RDP-XG, and RDP-starch.

2.5.3. Rheology Measurements. Rheology tests were done to analyze the mechanical properties of the hydrogels. A Bohlin Gemini HR Nano rheometer (Malvern Instruments) was used to perform the test under frequency sweep mode (0.01−100 Hz at 37 °C with a strain amplitude of 1%).

2.5.4. Fourier-Transform Infrared Spectroscopy (FTIR). FTIR spectra of pure XG, pure RDP, pure starch, RDP-starch, and RDP-XG were obtained with a Thermo Scientific Nicolet 6700 spectrometer with a universal attenuated total reflectance polarization accessory.

3. RESULTS AND DISCUSSION

3.1. Toxicity Analysis of RDP. In order for the flame-retardant hydrogel to further develop into cosmetic cream, all components of the hydrogel must be GRAS approved. The starch and XG powder used in this study are food grade GRAS compliant. Thus, only the toxicity of RDP needs to be evaluated. A total of 50,000 human dermal fibroblast cells were plated in a 24-well plate. After 24 h of incubation, 0.0001 v/v% to 0.003 v/v% of RDP was added directly into the culturing media. The cells were counted after 3 days, and the IC50 concentration, or the concentration at which 50% of the cells had died when RDP in the liquid form was added, was found to be 0.33 μg/mL (Figure 1).

Wang et al.,[10] previously demonstrated that when RDP was adsorbed onto bentonite clays, no cell toxicity was observed. Following the reaction model of Levchik et al.,[23,24] RDP was observed to undergo a dehydration reaction upon adsorption, releasing the phenol group, which was postulated to also reduce its toxicity to cells. Here, we produced a mixture of 30 wt % RDP and 70 wt % starch, which was stirred at 70 °C until the RDP was fully adsorbed onto the starch. The RDP-starch particles were then further heated for 24 h at 60 °C in a vacuum oven, to remove any traces of free phenol or other liquids. FTIR spectroscopy was employed to investigate the formation of hydrogen bonding between RDP and XG or starch particles. As depicted in Figure 2a, the spectrum of pure XG displayed a broad peak at around 3300 cm^{-1}, indicating the presence of O−H bonds in the alcohol groups of XG,[25] whereas pure RDP showed no absorption in this region. In the FTIR spectrum of RDP-XG, the transmittance curve exhibited a similar pattern, but the peak in the same region was broadened and had a higher absorbance rate. This is an indication of an increase in bond lengths of O−H covalent bonds due to their involvement in hydrogen bonding between RDP and XG.[26] Examination of RDP-starch yielded similar results, as depicted in Figure 2b. Again, the broadening and deepening of the transmittance curve between 3100 and 3600 cm^{-1} strongly suggest the existence of hydrogen bonding between RDP and starch.

To assess the toxicity of RDP after being absorbed onto the particle surface, human dermal fibroblasts (CF-31) were plated in tissue culture plastic dishes at a density of 10,000 cells/cm^2, cultured in full-DMEM media for 24 h, and exposed to either 0.4 or 0.1 mg/mL of starch and RDP-starch particles. The cells were fixed, and the actin was stained with Alexa Fluor 488

https://doi.org/10.1021/acs.biomac.1c00804
Biomacromolecules XXXX, XXX, XXX−XXX

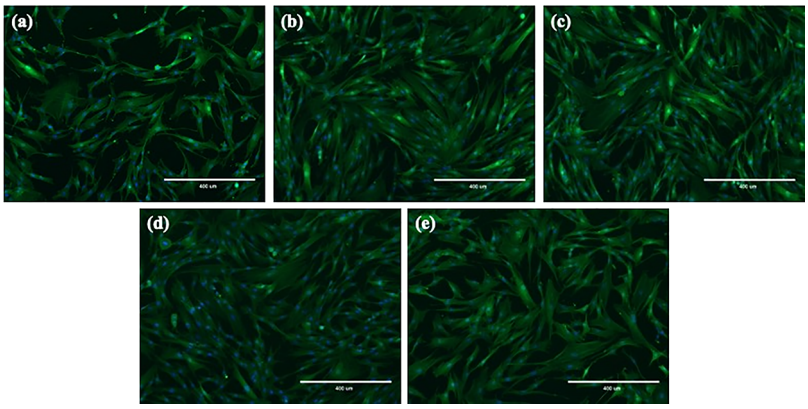

Figure 3. Human dermal fibroblast cell morphology study: (a) control; (b) cell grown on media with 0.1 mg/mL starch; (c) cell grown on media with 0.4 mg/mL starch; (d) cell grown on media with 0.1 mg/mL RDP-starch and (e) cell grown on media with 0.4 mg/mL RDP-starch. Scale bar is 400 μm on all images.

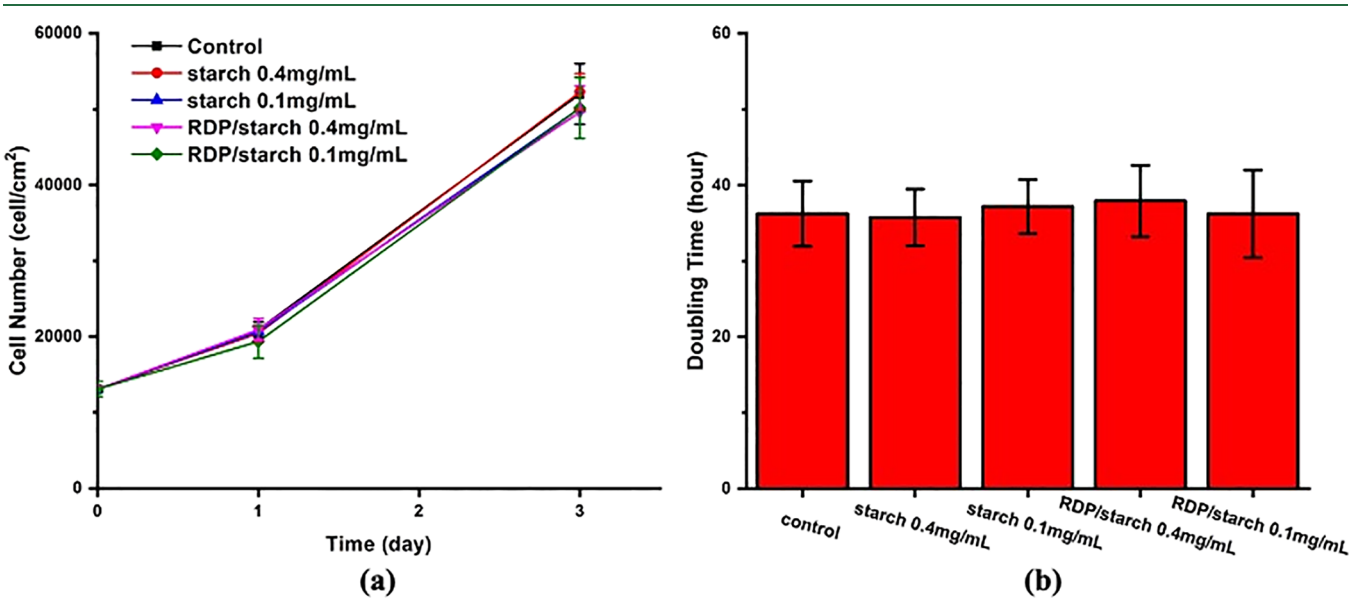

Figure 4. Human dermal fibroblast cell proliferation study: (a) cell proliferation curve; (b) doubling time of cells grown on media with different starch or RDP-starch concentrations.

phalloidin, while the nuclei were stained with DAPI. All cell cultures were confluent by the third day, as can be seen in Figure 3. The cells shown in the figure all had well extended actin, and no difference in cell morphology could be discerned in any of the cultures. Cell counts were also performed after 1 and 3 days in culture, and the data are shown in Figure 4a, from where we can see that the plating efficiency and the increase in cell numbers were indistinguishable between all cultures, regardless of the particle concentration added. The cell doubling times obtained from the data are shown in Figure 4b, where no significant differences are observed between any of the cultures and the control. From these data, we can conclude that for the concentrations of the particles used, no discernible damage occurs to the dermal fibroblasts, even though the maximum RDP concentration added was approximately 0.12 mg/mL or at least two orders of magnitude larger than the IC50 value obtained for the pure RDP liquid. Further in vivo experimentation must still be performed before these particles can obtain GRAS designation, but these results are in good agreement with prior work with RDP adsorbed on clays and hence confirm the hypothesis that the toxicity is mitigated upon removal of the phenolic group.

3.2. Rheology. Application of the cream is very important, and hence, the rheological properties have to be optimized for ease of spreading. In Figure 5, we plot the viscosity of the gels as a function of shear rate, where we find that the XG gels are highly thixotropic,[27] where the viscosity decreases drastically with an increase of shear rate. From the figure, we can also see that relative to a pure XG gel, addition of RDP-soaked starch results in an increase in viscosity in agreement with previous reports,[16] and addition of RDP adsorbed to XG decreases the viscosity. Hence, the two effects nearly balance with the overall viscosity of the formulated gel being nearly the same as pure XG.

3.3. Flammability Analysis. *3.3.1. Thermal Imaging of the Burning Process.* To observe the temperature change on the sample surface when exposed to extreme heat, an infrared thermal camera was used to take thermal images at various time points during the burning test, as shown in Figure 6. Since the upper limit of the thermal camera's temperature range is 280 °C, regions that have a temperature higher than 280 °C

https://doi.org/10.1021/acs.biomac.1c00804
Biomacromolecules XXXX, XXX, XXX−XXX

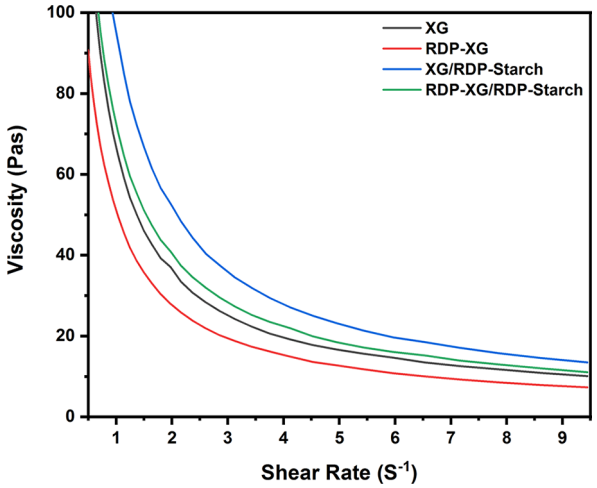

Figure 5. Rheology test result of the hydrogels.

will appear as a bright spot on the image. The first row of images in Figure 6 shows the control sample of chick tissue covered with the pure XG hydrogel. We could see that the bright spot on the sample surface kept expanding with the burning process, which is in agreement with the previous observation where the pure XG gel lost its protection once all water has evaporated and the dried XG gel burned away almost immediately. Thermal images of the sample covered by FireIce are shown in the second row in Figure 6. Compared to the images of the control pure XG hydrogel, the bright spots in the images of FireIce are all smaller, which indicates that the FireIce has a better thermal protection than the control XG gel. However, the area of the bright spot also kept enlarging as the burning continues, which corresponds to the previous result that the FireIce loses its protection with the water evaporation. On the contrary, in the thermal images of the RDP-XG/RDP-starch hydrogel-covered sample, shown in the third row, the bright spot on the sample surface becomes smaller instead of larger. Moreover, by the end of the burning process at 150 s, the bright spot almost disappeared, which means that the sample surface was burning at a lower temperature than the other samples. This effect can be ascribed to the char formation on the RDP-XG/RDP-starch hydrogel surface, which separates the hydrogel and tissue sample from the heat of the torch flame. As a result, both the burning of the hydrogel and evaporation of water were suppressed, which greatly reduced the temperature of the sample surface. This result also correlates with the previous observation that the temperature on the inside of the tissue with the coverage of the RDP-XG/RDP-starch hydrogel is much lower than that for the other samples by the end of the burning test.

3.3.2. Exposure to Open Flame. A model setup was first developed in order to test the degree of protection afforded by the gel, which is shown in Figure 7. A section of raw chicken

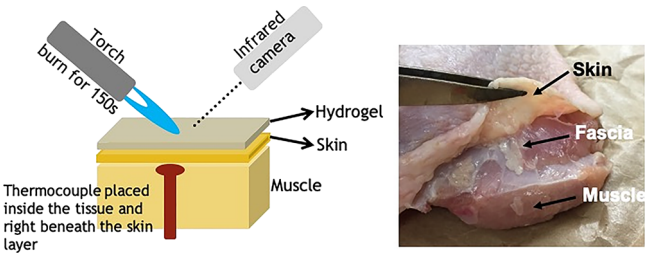

Figure 7. Schematic of the burning test experimental setup and result of the burning test comparison between hydrogels and the commercial product.

thigh, complete with muscle, fascia, and skin, was placed directly on a metal plate with a rectangular opening. A type J thermocouple was inserted through the opening and threaded through the thigh muscle to the fascia, just below the skin. Burning was affected by bringing a propane torch flame in direct contact with the top of the sample for 2.5 min, while the temperature was recorded as a function of time with the thermocouple, and the top of the sample was imaged with the infrared camera. Four types of hydrogels were tested: (a) a 97.5 wt % water/XG gel, (b) the 2.5% RDP-XG and RDP-starch blend, (c) FireIce, a commercial nonbiodegradable, formulated base on surfactant-modified polyacrylamide, and (d) a control sample without application of any gel. In Figure 8, we plot the increase in temperature as a function of time for the four different samples.

From the figure, we find that the curves, and especially the control (without gel), are more complex than a simple linear fit. Without a detailed knowledge of the multiple factors involved, we approximate the curves by fitting with two linear curves having different slopes. The values of the slopes and the differences between them are tabulated in Table 2 where we find that the steepest rate of increase with time occurs in the sample without gel, the rate of increase decreases with the addition of the XG gels and FireIce, but the largest decrease occurs with the addition of the RDP/XG formulation. Since the torch provides a constant source of heat flux, the change in

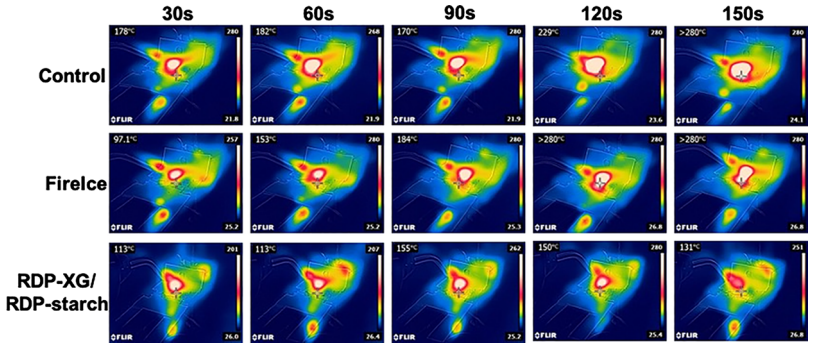

Figure 6. Top view thermal images taken during application of the torch to the bare chicken skin samples (control), and samples covered with FireIce or the other hydrogel.

https://doi.org/10.1021/acs.biomac.1c00804
Biomacromolecules XXXX, XXX, XXX−XXX

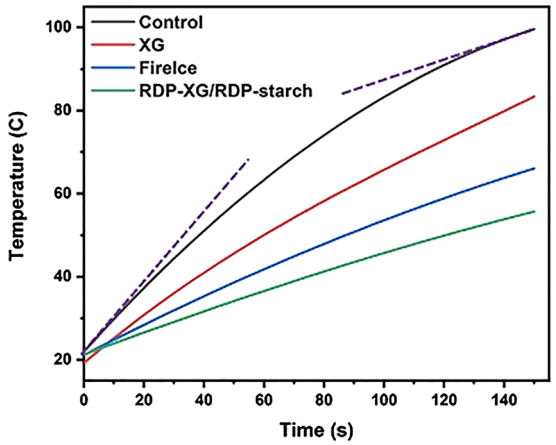

Figure 8. Temperature change inside chicken tissue during the burning test.

Table 2. Slope Change of the Temperature vs Time Curve of the Burning Process

	slope 1	slope 2	difference
control	0.75	0.26	0.49
XG	0.56	0.35	0.21
FireIce	0.36	0.24	0.12
RDP-XG/RDP-starch	0.26	0.19	0.07

the slope denotes a change in the heat conduction properties of the material being burned. Hence, in the control sample, both skin and muscle burn, each having a different heat capacity and hence slopes. In the case of XG and FireIce, first, the hydrogel burns followed by skin and then muscle. In the case of our formulation, most of the heat is still dissipated by the gel and hence the slowest increase in temperature. In Figure 9, we show optical images of the tissue and the control without cream and the other three samples with volume equivalent layers of the creams. Before application of the torch, one can clearly see the different layers, skin, fascia, and muscle on the tissue. After burning, we can see that a thick black char is formed on all samples. On the control sample, the charred segment is mostly skin, facia, and the upper layer of the muscle. On the XG sample and FireIce samples, we observe a char layer, which is easily removed from the sample, ostensibly the charred, but after 150 s, the skin is charred as well. On the XG sample, a char layer also forms on the upper half of the muscle, while on the FireIce sample, a thinner char layer is observed, but the entire muscle layer is damaged as well. In sharp contrast on the sample with RDP and XG, the heavy char layer is easily removed leaving behind unperturbed tissue. This is further emphasized in the enlarged image, shown in Figure 9a,b, where the skin is lifted with tweezers to illustrate that the layers under the gel are intact skin, fascia, and muscle.

These calculations are further confirmed by photographic images of the chicken tissue after burning. In Figure 9, on the left, we show the control tissue sample after 150 s of burning, with only the XG hydrogel. From the figure, we see that the tissue is heavily burned, which is consistent with the measured temperature of 83.4 °C at the end of the burning. When the sample covered by FireIce was exposed to the torch flame, extensive steam was generated from the FireIce hydrogel, which conducted heat away from the sample, lowering the sample temperature. However, once all the water evaporated, the hydrogel protection was gone, and the sample was also heavily burned, and the skin layer was blackened. In both cases, the behavior of the gels is consistent with the two slope curves observed, where one slope corresponds to the specific heat, while the gel layer is still there, and the second slope corresponds to the specific heat of the tissue, which now absorbs the entire flux and will soon burn. A different response is apparent when burning the sample covered with the RDP-XG/RDP-starch hydrogel. In addition to the protective aspect of the water, a char layer is quickly formed on the hydrogel surface, which maintains its structure throughout the entire burning process. The char layer is the result of a chemical reaction between RDP, which decomposes during combustion into polyphosphoric acid that in turn reacts with any surface carbon source. In the case of our RDP-XG/RDP-starch hydrogel, both XG and starch provide the carbon source, accelerating char formation, after the water evaporates. Formation of the char layer protects the skin from burning; first, since it is an endothermic reaction, heat is removed, while the char forms, as we can see in Figure 6, where the entire burning process occurs at a cooler temperature. Second, the char forms a barrier to heat propagation directly to the skin, decreasing the slope observed in Figure 7 and protecting the chicken skin and tissue from the heat of the flame. As a result, the highest temperature of the sample was recorded as 55.7 °C by the end of the burning test, which is a 34% reduction compared to the control sample and 16% reduction compared to the commercial FireIce. After the test, the char layer was

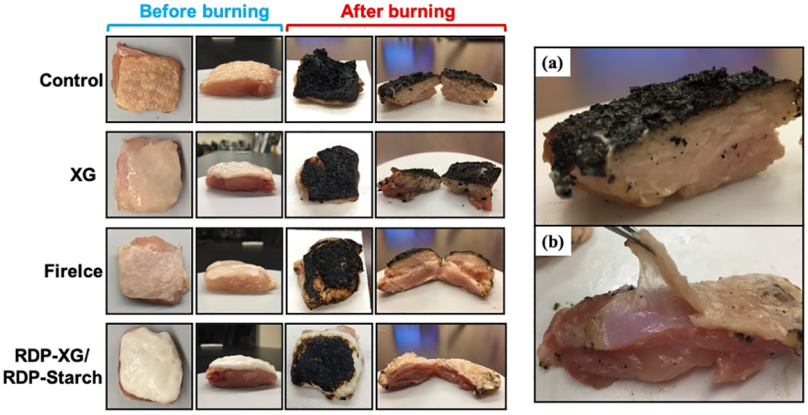

Figure 9. Optical images of chicken tissue samples covered with different hydrogels before and after the burning test.

https://doi.org/10.1021/acs.biomac.1c00804
Biomacromolecules XXXX, XXX, XXX−XXX

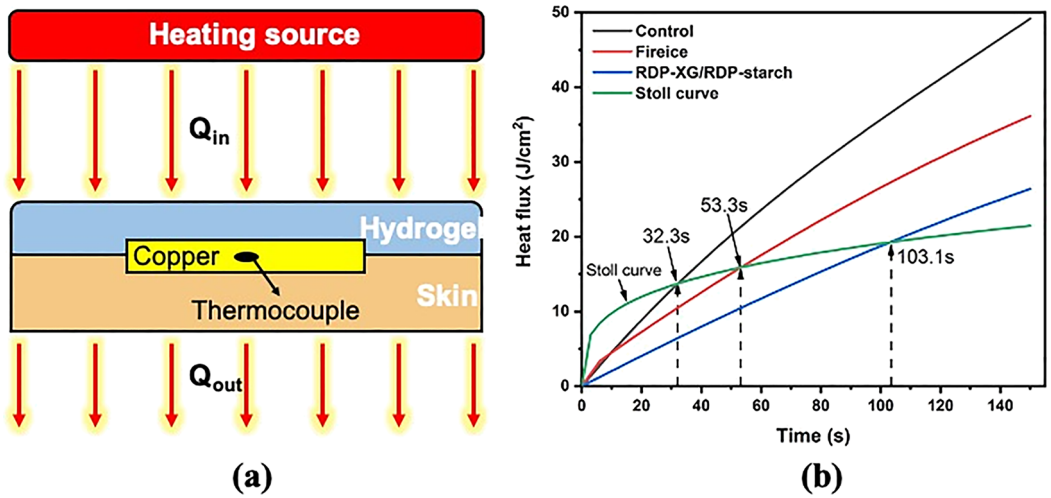

Figure 10. (a) Illustration of the thermal protective performance (TPP) test setup; (b) thermal protective performance test result of the pure XG hydrogel (black line), FireIce (red line), and RDP-XG/RDP-starch hydrogel (blue line). Comparison to the Stoll curve (green line).

lifted off the sample to observe the chicken skin and tissue, which were both found as intact with hydrogel residues still covering the sample surface. Thus, we could see that the RDP-XG/RDP-starch hydrogel is a flame retardant, which forms char when in contact of direct flame and provides protection for skin underneath.

3.3.3. Thermal Protective Performance Test. In the case of the propane torch, even though we had measured the temperature/time profile, the heat flux from the source was difficult to quantify. In order to obtain a more quantitative analysis of the thermal insulating effect of our flame-retardant hydrogel, the thermal protective performance (TPP) test was performed on the pure XG hydrogel, commercial FireIce, and the RDP-XG/RDP-starch hydrogel. Figure 10a shows the illustration of the TPP test setup. First, the temperature of the sample surface was recorded as a function of time. Then, the heat transfer through the hydrogel to the skin surface was calculated from the temperature change with the equation:

$$Q\ (\mathrm{J/cm^2}) = \frac{m \times C \times (T_{\mathrm{final}} - T_{\mathrm{initial}})}{A}$$

where m is the mass of the copper calorimeter, C is the specific heat of the copper, and A is the area of the copper calorimeter. Then, TPP test results of the three hydrogels were compared with the Stoll curve, which represents the approximate second-degree burn injury time point on continuous heating without accounting for the energy remaining in the specimen. Second-degree burns would affect the epidermis and the dermis and cause pain, swelling, and blistering. The Stoll curve is calculated by the equation below:[28]

$$\text{Stoll curve}\ (\mathrm{J/cm^2}) = 5.0204 \times t_i^{0.2901}$$

where t is the time. The comparison of the TPP test result is shown in Figure 10b. Since the Stoll curve represents the duration needed for a specific heat flux to cause a second-degree burn, the area under the Stoll curve is considered as safe, and the intersection point of the heat flux curve of the hydrogel and the Stoll curve indicates the hydrogels' maximum protection time against second-degree burns. As we can see, the pure XG hydrogel could only provide protection up to 32.3 s. The commercial FireIce could protect the skin for up to 53.3 s due to the evaporation of water, which takes away the heat accumulated on the skin surface. Once all water in FireIce was evaporated, the gel lost its protection. The RDP-XG/RDP-starch hydrogel could provide up to 103 s, which is double that for the FireIce and triple the protection time of the control XG hydrogel. The prolonged protection time is caused by the char layer formed on the hydrogel surface, which blocked the heat transferring onto the skin surface.

4. CONCLUSIONS

We have succeeded in producing a flame-retardant hydrogel formulation with biodegradable ingredients, which can be applied directly onto skin and prevent injuries for first responders to a fire. The hydrogel was formulated using mostly GRAS compliant materials. The toxicity of the only non-GRAS component was tested on primary dermal fibroblast tissue cultures. RDP alone when added to the cell culture was toxic (IC50), killing more than half of the culture at a concentration of 0.33 μg/mL. On the other hand, when RDP was first adsorbed onto starch forming the particles used in our formulation, no toxicity was observed at any concentration, and the cells proliferated normally. Burning of the XG/RDP/ gel indicated a high degree of charring, and FTIR spectroscopy showed clear indication of hydrogen bonding between the RDP and the starch carrier matrix. Hence, the formulated hydrogel protected from fire not only by providing water but also via endothermic chemical reactions, which further decrease the temperature of the burn area. The efficacy of the gel was tested by burning chicken tissue obtained commercially with a propane torch and monitoring the temperature with an FLIR thermal camera and a thermocouple placed directly beneath the skin. The rise in temperature with time was the longest with our formulation as compared to only XG or FireIce, and optical examination of the tissue indicated that all samples, except the one protected with our formulations, had burned through skin, fascia, and muscle layers. Our sample had not sustained any damage that we could observe. To further analyze the hydrogel's thermal insulating effect in a more quantitative manner, the TPP test was done. In addition, the results are in agreement with the previous burning test. When compared with the Stoll curve, which indicates the onset of second-degree burn, the RDP-XG/RDP-starch hydrogel could provide a protection time that

https://doi.org/10.1021/acs.biomac.1c00804
Biomacromolecules XXXX, XXX, XXX−XXX

is three times longer than that for the pure XG hydrogel and twice longer than that for the commercial FireIce. Moreover, rheology test results confirmed the shear thinning behavior of the RDP-XG/RDP-starch hydrogel. Thus, this hydrogel composite could be a promising formulation for development of antiburn cream.

AUTHOR INFORMATION

Corresponding Authors

Yuan Xue − *Department of Materials Science and Chemical Engineering, Stony Brook University, Stony Brook, New York 11794, United States; ThINC Facility at Stony Brook University, Stony Brook, New York 11794, United States;* orcid.org/0000-0002-5613-8688; Email: yuan.xue@stonybrook.edu

Miriam Rafailovich − *Department of Materials Science and Chemical Engineering, Stony Brook University, Stony Brook, New York 11794, United States;* Email: miriam.rafailovich@stonybrook.edu

Authors

Fan Yang − *Department of Materials Science and Chemical Engineering, Stony Brook University, Stony Brook, New York 11794, United States*

Juyi Li − *Department of Materials Science and Chemical Engineering, Stony Brook University, Stony Brook, New York 11794, United States*

Xianghao Zuo − *Department of Materials Science and Chemical Engineering, Stony Brook University, Stony Brook, New York 11794, United States;* orcid.org/0000-0002-9372-5136

Bole Pan − *Columbia College, Columbia University, New York, New York 10027, United States*

Mingkang Li − *The School of Computer Science, Carnegie Mellon University, Pittsburgh, Pennsylvania 15213, United States*

Lisa Quinto − *Department of Materials Science and Chemical Engineering, Stony Brook University, Stony Brook, New York 11794, United States*

Jalaj Mehta − *Hauppauge High School, Hauppauge, New York 11788, United States*

Lauren Stiefel − *Yeshiva University High School for Girls, Hollis wood, New York 11423, United States*

Conor Kimmey − *Department of Materials Science and Chemical Engineering, Stony Brook University, Stony Brook, New York 11794, United States*

Yuval Eshed − *Department of Mechanical Engineering, Technion Israel Institute of Technology, Haifa 3200003, Israel*

Eyal Zussman − *Department of Mechanical Engineering, Technion Israel Institute of Technology, Haifa 3200003, Israel*

Marcia Simon − *Department of Oral Biology and Pathology, Stony Brook University, Stony Brook, New York 11794, United States*

Complete contact information is available at: https://pubs.acs.org/10.1021/acs.biomac.1c00804

Author Contributions

The manuscript was written through contributions of all authors. All authors have given approval to the final version of the manuscript.

Notes

The authors declare no competing financial interest.

ACKNOWLEDGMENTS

The authors acknowledge the support from the Stony Brook Foundation/Edward Weil Grant and the Louis Morin Charitable Trust. We would also like to acknowledge the NY State Center for Advanced Technology and ICL Industrial Products.

REFERENCES

(1) Kahn, S. A.; Patel, J. H.; Lentz, C. W.; Bell, D. E. Firefighter burn injuries: predictable patterns influenced by turnout gear. *J. Burn Care Res.* **2012**, *33*, 152−156.

(2) Richard Campbell, B. E., Molis, J.L. *United States Firefighter Injury Report 2018*; National Fire Protection Association (NFPA): NFPA Journal, 2019.

(3) Hoffman, A. S. Hydrogels for biomedical applications. *Adv. Drug Deliv. Rev.* **2012**, *64*, 18−23.

(4) Seliktar, D. Designing cell-compatible hydrogels for biomedical applications. *Science* **2012**, *336*, 1124−1128.

(5) Hyon, S.-H.; Cha, W.-I.; Ikada, Y.; Kita, M.; Ogura, Y.; Honda, Y. Poly (vinyl alcohol) hydrogels as soft contact lens material. *J. Biomater. Sci. Polym. Ed.* **1994**, *5*, 397−406.

(6) Carballo-Molina, O. A.; Velasco, I. Hydrogels as scaffolds and delivery systems to enhance axonal regeneration after injuries. *Front. Cell. Neurosci.* **2015**, *9*, 13.

(7) Worthington, P.; Pochan, D. J.; Langhans, S. A. Peptide hydrogels−versatile matrices for 3D cell culture in cancer medicine. *Front. Oncol.* **2015**, *5*, 92.

(8) Das, S.; Baker, A. B. Biomaterials and nanotherapeutics for enhancing skin wound healing. *Front. Bioeng. Biotechnol.* **2016**, *4*, 82.

(9) Sun, G.; Zhang, X.; Shen, Y.-I.; Sebastian, R.; Dickinson, L. E.; Fox-Talbot, K.; Reinblatt, M.; Steenbergen, C.; Harmon, J. W.; Gerecht, S. Dextran hydrogel scaffolds enhance angiogenic responses and promote complete skin regeneration during burn wound healing. *Proc. Natl. Acad. Sci. U. S. A.* **2011**, *108*, 20976−20981.

(10) Wang, T.; Zhu, X.-K.; Xue, X.-T.; Wu, D.-Y. Hydrogel sheets of chitosan, honey and gelatin as burn wound dressings. *Carbohydr. Polym.* **2012**, *88*, 75−83.

(11) Illeperuma, W. R. K.; Rothemund, P.; Suo, Z.; Vlassak, J. J. Fire-Resistant Hydrogel-Fabric Laminates: A Simple Concept That May Save Lives. *ACS Appl. Mater. Interfaces* **2016**, *8*, 2071−2077.

(12) Van Vlierberghe, S.; Dubruel, P.; Schacht, E. Biopolymer-based hydrogels as scaffolds for tissue engineering applications: a review. *Biomacromolecules* **2011**, *12*, 1387−1408.

(13) Thakur, V. K.; Thakur, M. K. Recent advances in green hydrogels from lignin: a review. *Int. J. Biol. Macromol.* **2015**, *72*, 834−847.

(14) García-Ochoa, F.; Santos, V. E.; Casas, J. A.; Gómez, E. Xanthan gum: production, recovery, and properties. *Biotechnol. Adv.* **2000**, *18*, 549−579.

(15) Katzbauer, B. Properties and applications of xanthan gum. *Polym. Degrad. Stab.* **1998**, *59*, 81−84.

(16) Abdulmola, N. A.; Hember, M. W. N.; Richardson, R. K.; Morris, E. R. Effect of xanthan on the small-deformation rheology of crosslinked and uncrosslinked waxy maize starch. *Carbohydr. Polym.* **1996**, *31*, 65−78.

(17) Veiga-Santos, P.; Oliveira, L. M.; Cereda, M. P.; Alves, A. J.; Scamparini, A. R. P. Mechanical properties, hydrophilicity and water activity of starch-gum films: effect of additives and deacetylated xanthan gum. *Food Hydrocolloids* **2005**, *19*, 341−349.

(18) Leone, G.; Consumi, M.; Lamponi, S.; Bonechi, C.; Tamasi, G.; Donati, A.; Rossi, C.; Magnani, A. Hybrid PVA-xanthan gum hydrogels as nucleus pulposus substitutes. *Int. J. Polym. Mater.* **2019**, *68*, 681−690.

(19) Guo, Y.; He, S.; Zuo, X.; Xue, Y.; Chen, Z.; Chang, C.-C.; Weil, E.; Rafailovich, M. Incorporation of cellulose with adsorbed

phosphates into poly (lactic acid) for enhanced mechanical and flame retardant properties. *Polym. Degrad. Stab.* **2017**, *144*, 24−32.
(20) Jiang, Z.; Liu, S.; Zhao, J.; Chen, X. Flame-retarded mechanism of SEBS/PPO composites modified with mica and resorcinol bis (diphenyl phosphate). *Polym. Degrad. Stab.* **2013**, *98*, 2765−2773.
(21) Pack, S.; Kashiwagi, T.; Cao, C.; Korach, C. S.; Lewin, M.; Rafailovich, M. H. Role of surface interactions in the synergizing polymer/clay flame retardant properties. *Macromolecules* **2010**, *43*, 5338−5351.
(22) Murashko, E. A.; Levchik, G. F.; Levchik, S. V.; Bright, D. A.; Dashevsky, S. Fire Retardant Action of Resorcinol Bis(Diphenyl Phosphate) in a PPO/HIPS Blend. *J. Fire Sci.* **1998**, *16*, 233−249.
(23) Levchik, S. V.; Weil, E. D. A review of recent progress in phosphorus-based flame retardants. *J. Fire Sci.* **2006**, *24*, 345−364.
(24) Levchik, S. V.; Bright, D. A.; Alessio, G. R.; Dashevsky, S. New halogen-free fire retardant for engineering plastic applications. *J. Vinyl Addit. Technol.* **2001**, *7*, 98−103.
(25) Sheppard, N., Infrared Spectroscopy And Hydrogen Bonding — Band-Widths And Frequency Shifts. In *Hydrogen Bonding*, Hadži, D., Ed. Pergamon: 1959; 85−105.
(26) Wang, F. C.; Feve, M.; Lam, T. M.; Pascault, J.-P. FTIR analysis of hydrogen bonding in amorphous linear aromatic polyurethanes. II. Influence of styrene solvent. *J. Polym. Sci., Part B: Polym. Phys.* **1994**, *32*, 1315−1320.
(27) Tan, E.; Yeong, W. Y., *Direct Bioprinting of Alginate-Based Tubular Constructs Using Multi-Nozzle Extrusion-Based Technique*. In 1st Int. Conf. on Prog. in Addit. Manuf., Singapore, 2014.
(28) Stoll, A. M.; Chianta, M. A. Method and rating system for evaluation of thermal protection. *Aerosp. Med.* **1969**, *40*, 1232−1238.

https://doi.org/10.1021/acs.biomac.1c00804
Biomacromolecules XXXX, XXX, XXX−XXX